

Rovibrational averaging of nuclear shielding in MX_6 -type molecules

Cynthia J. Jameson

Department of Chemistry, University of Illinois at Chicago, Chicago, Illinois 60680

A. Keith Jameson

Department of Chemistry, Loyola University, Chicago, Illinois 60626

(Received 10 July 1986; accepted 14 August 1986)

Calculations of the mean M–X bond displacements in octahedral MX_6 molecules by the L tensor and Bartell methods using anharmonic force fields for SF_6 , SeF_6 , TeF_6 , WF_6 , PtCl_6^- , and PtBr_6^- are compared with electron diffraction data in SF_6 , and are used in the interpretation of ^{19}F , ^{77}Se , ^{125}Te , and ^{195}Pt chemical shifts in these molecules. The temperature and mass dependence of M and X chemical shifts can be written in terms of $\langle\Delta r_{\text{MX}}\rangle$, and the two together provide a critical test of anharmonic force fields. The direct proportionality of the isotope shifts to the mass factor $(m' - m)/m'$ is found to be a direct consequence of the calculated linear dependence of $\langle\Delta r\rangle - \langle\Delta r\rangle'$ and $\langle(\Delta r)^2\rangle - \langle(\Delta r)^2\rangle'$ on this mass factor. The observed isotope shifts and temperature dependent chemical shifts in the zero pressure limit can be used to determine the sensitivity of the nuclear magnetic shielding to bond extension.

INTRODUCTION

The effects of anharmonicity of vibration become evident in temperature dependent studies of electronic properties, such as NMR chemical shifts in the zero pressure limit, and in the internuclear distances obtained from electron diffraction studies of hot molecules. Anharmonicities also shift and split excited vibrational levels and cause resonances between them. Model potential surfaces which are used to predict the vibration–rotation structure of hot bands, combination bands, and overtones can be used to calculate the mean bond displacements with which temperature-dependent electron diffraction and NMR shift data can be interpreted. Two such model potentials have recently been proposed for SF_6 by Krohn and Overend and by Stanton and Bartell.^{1,2} Both include explicitly a Morse potential in each of the S–F bonds and an explicit Urey–Bradley interaction between 12 nearest neighbor nonbonded pairs of F atoms. In one model bend–bend–bend constants are explicitly included.² A third set of anharmonic force field parameters have been obtained directly from spectroscopic constants, including only the stretching anharmonicity.³

In this paper, these model potentials are used to calculate the mean S–F bond length and mean square amplitudes. The Stanton and Bartell model is also used for the calculations of Se–F, Te–F, W–F, Pt–Cl, and Pt–Br mean bond displacements in various isotopomers of SeF_6 , TeF_6 , WF_6 , PtCl_6^- , and PtBr_6^- . The results are compared with the simple Bartell model for AX_6 molecules. The experimental NMR data of the preceding paper (the temperature dependence of the M and the ^{19}F shifts and the M-induced ^{19}F isotope shifts) are interpreted in terms of the calculated rovibrational averages.⁴ The magnitudes and the linear dependence of the isotope shifts on the mass factor $(m' - m)/m'$ are accounted for. The model is extended to PtCl_6^- and PtBr_6^- to account for the $^{37/35}\text{Cl}$ and $^{81/79}\text{Br}$ -induced ^{195}Pt shifts and the temperature dependence of ^{195}Pt shifts.

CALCULATION OF MEAN BOND DISPLACEMENTS

The model potential that we have adopted for all molecules in this work is that proposed by Stanton and Bartell,² which has general features in common with that of Krohn and Overend.¹ In this model we start with a set of the quadratic GHFF terms which is required to bring the harmonic potential into agreement with experiment. The contributions to anharmonicities are (a) the implicit anharmonicity arising from the nonlinear transformation of the GHFF potential to normal coordinates, (b) an explicit Morse potential between bonded atoms in the molecule, (c) an explicit Urey–Bradley interaction between the 12 nearest neighbor nonbonded pairs of F atoms, and (d) bend–bend–bend anharmonicities such as those introduced by a POS model which was found necessary and satisfactory in accounting for the mean displacements of geminal nonbonded distances. We leave out the last contribution because it has been shown that the bonded distances are not sensitive to bending anharmonicity,⁵ and the NMR data we wish to interpret are largely dependent on bonded distances. With this model, the cubic force constants in curvilinear internal coordinates are given by

$$\begin{aligned} \Delta r_1^3: & \quad \tilde{f}_{rrr} = (F_3 + 3F - 3F')/r_e - 3aK, \\ \Delta r_1^2 \Delta r_2: & \quad \tilde{f}_{rrr}' = (F_3 + 3F - 3F')/4r_e, \\ (r_e \Delta \alpha)^3: & \quad \tilde{f}_{aaa} = (F_3 - 3F - F')/4r_e, \\ \Delta r_1^2 (r_e \Delta \alpha): & \quad \tilde{f}_{rra} = (F_3 + 3F - 3F')/4r_e, \\ \Delta r_1 \Delta r_2 (r_e \Delta \alpha): & \quad \tilde{f}_{rr'a} = (F_3 + F + 3F')/4r_e, \\ \Delta r_1 (r_e \Delta \alpha)^2: & \quad \tilde{f}_{raa} = (F_3 + F - F')/4r_e. \end{aligned} \quad (1)$$

Krohn and Overend use $-6a^3 D_M$ instead of $-3aK$.

We use Stanton and Bartell's parameters for SeF_6 and TeF_6 . The model potential parameters of Krohn and Overend for SF_6 are different from those given by Stanton and

Bartell in that the reference distance and the bond dissociation energy D_M in the Morse function are taken to be adjustable parameters, as are the Morse parameter a and the nonbonded distance parameter q_0 . The complete set of parameters are specified by imposing consistency with experiment in the derivatives of the total stretching potential and by minimizing deviations from eleven experimental anharmonicity constants. Application of this technique to other MF₆ molecules is only possible if the set of anharmonicity constants are available from experiment. This is unfortunately not the case except for SF₆. For WF₆, PtCl₆[−], and PtBr₆[−] we have less complete information. We choose F' , F , and F_3 for WF₆ by the usual recipe: $F' \simeq -0.1 F$ and $F_3 \simeq -10 F$, with F being determined by the F_{34} symmetry force constant. For PtCl₆[−] and PtBr₆[−] we choose Lennard-Jones nonbonded potentials for Cl-Cl and Br-Br interactions simulated by the Ar-Ar and Kr-Kr potentials.⁶ The q_0 and ϵ for the latter are not significantly different from those found earlier in fitting F values of various chlorides and bromides.⁷ The Morse parameter a is calculated from the WF bond dissociation energy, and the Urey-Bradley stretching parameter K from the comparative studies of MX₆ force fields.⁸ For the Pt-Cl and Pt-Br bonds a was estimated by using Herschbach and Laurie's constants for representative elements.⁹ These constants are not quite appropriate for transition elements but no better estimate is available at the present time. The parameters used in this work are given in Table I. The cubic force constants in internal coordinates are given in Table II. Cubic force constants involving internal coordinates which do not share a common bond are set to zero, and interactions between opposite stretching bonds are also set to zero, although the latter have been found to be significant in SF₆.³

The mean bond displacements $\langle \Delta r \rangle$ are calculated by the method of Bartell¹⁰ which we have implemented for several molecular types.¹¹ In this case it takes the form

$$\langle \Delta r \rangle = F^{-1} \Sigma, \quad (2)$$

where F^{-1} is the inverse of the 6×6 force constant matrix F in internal coordinates including the stretches only. The vector Σ contains the sums

$$\begin{aligned} \Sigma_k = & \sum_{i=1}^6 \sum_{j=7}^{18} \frac{F(i,j)}{2r_e} \langle \mathfrak{J}_i \mathfrak{J}_j \rangle \epsilon_{kj} \\ & + \sum_{i=7}^{18} \sum_{j=7}^{18} \frac{F(i,j)}{4r_e} \langle \mathfrak{J}_i \mathfrak{J}_j \rangle (\epsilon_{ki} + \epsilon_{kj}) \\ & + \sum_{i=1}^{18} \sum_{j=1}^{18} \frac{-F(i,j,k)}{2} \langle \mathfrak{J}_i \mathfrak{J}_j \rangle. \end{aligned} \quad (3)$$

For $k = 1$ to 6, $\epsilon_{kj} = 1$ if the k th atom is involved in the curvilinear internal coordinate \mathfrak{J}_j otherwise it is zero. $F(i,j)$ are the 18×18 F matrix elements and $F(i,j,k)$ are the cubic force constants in curvilinear internal coordinates in Table II. These do not involve the atomic masses in any way and are therefore the same for different isotopic species. All the mean square amplitudes $\langle \mathfrak{J}_i \mathfrak{J}_j \rangle$ including angles, are included in Eq. (3), calculated using standard techniques described earlier.¹¹

$$\langle \mathfrak{J} \mathfrak{J} \rangle = \tilde{U} L \langle Q^2 \rangle \tilde{L} U. \quad (4)$$

Only the last terms in Eq. (3) are due to the explicit cubic force constants $F(i,j,k)$ introduced by the Morse anharmonicity and the nonbonded interactions. The first two terms depend only on the quadratic internal force constants and contribute to $\langle \Delta r \rangle$ due to the nonlinear transformation between the curvilinear internal coordinates Δr_i and the normal coordinates, and may be viewed as curvilinear correction terms.

Alternatively the mean bond displacements may be calculated using the method of Hoy, Mills, and Strey,¹²

$$\mathfrak{J} = L^* Q. \quad (5)$$

The L tensor elements are the first, second, third,... derivatives of the internal coordinates with respect to the normal coordinates Q taken at equilibrium. The high symmetry of MX₆-type molecules allows the L tensor elements to be written explicitly in terms of the L matrix elements in the symmetry coordinates.³ For the MX bond in MX₆-type molecules, symmetry reduces Eq. (5) to

$$\langle \Delta r \rangle = \frac{1}{\sqrt{6}} \left\{ L_{11} \langle Q_1 \rangle + \frac{1}{2} \sum_{s=1}^{15} L_1^{ss} \langle Q_s^2 \rangle + \dots \right\}, \quad (6)$$

TABLE I. Parameters used in these calculations.

	Observed freq. Ref.	GHFF Ref.	r_e (Å) and Ref.	a (Å ^{−1}) and Ref.	K (mdyn Å ^{−1}) and Ref.	F'	F (mdyn Å ^{−1})	F_3	Ref.
SF ₆	27	1	1.5561, 1	1.8, 2	3.63, 2	−0.125	1.032	−8.51	2
SeF ₆	27	30	1.680, 2	1.9, 2	3.96, 2	−0.058	0.518	−4.62	2
TeF ₆	27	31	1.811, 2	2.1, 2	4.59, 2	−0.028	0.267	−2.58	2
WF ₆	28	28	1.832, 32	1.495 ^a	3.79, 8	−0.021	0.21	−2.1	c
PtCl ₆ [−]	7, 29	8	2.334, 33	1.25 ^b	1.86, 7	−0.006	0.10 ^c	−1.62	d
PtBr ₆ [−]	7, 29	8	2.484, 33	1.386 ^b	1.54, 7	−0.007	0.13 ^f	−2.08	d

^a Calculated from $a = K/2D_e$, using $D_0 = 121$ kcal (Ref. 34).

^b Calculated using r_e and Herschbach and Laurie parameters for representative elements (Ref. 9).

^c $F' = -0.1 F$, $F_3 = -10 F$ assumed, and F calculated from symmetry force constant F_{34} .

^d Calculated using a Lennard-Jones potential with $q_0 = 3.759$ Å, $\epsilon = 143.22$ deg for Cl-Cl and $q_0 = 4.018$ Å, $\epsilon = 197.04$ deg for Br-Br (Ref. 6).

^e Compare with 0.15 from Ref. 8.

^f Compare with 0.14 from Ref. 8.

TABLE II. Cubic force constants in curvilinear internal coordinates, in mdyn Å⁻².

	SF ₆ ^a	SF ₆	SeF ₆	TeF ₆	WF ₆	PtCl ₆ ⁼	PtBr ₆ ⁼
\tilde{f}_{rrr}	-32.964	-22.840	-24.293	-29.853	-18.454	-7.53	-7.074
$\tilde{f}_{rrr}^{\text{cis}}$	-1.574	-1.553	-0.773	-0.397	-0.261	-0.185	-0.223
\tilde{f}_{aaa}	-1.7595	-1.844	-0.910	-0.463	-0.198	-0.205	-0.248
\tilde{f}_{rra}	-1.1529	-0.8010	-0.430	-0.234	-0.364	-0.139	-0.168
$\tilde{f}_{r'r\alpha}$	-1.390	-1.262	-0.636	-0.331	-0.324	-0.164	-0.198
\tilde{f}_{raa}	-1.3636	-1.181	-0.602	-0.315	-0.312	-0.162	-0.195

^aReference 1.

where

$$\langle Q_1 \rangle = -\frac{1}{4} (h/4\pi^2 c)^{1/2} \omega_1^{-3/2} \times \sum_{s=1}^{15} \phi_{1ss} \coth(hc\omega_s/2kT). \quad (7)$$

ϕ_{1ss} are the cubic force constants in dimensionless normal coordinates, obtained from the force constants in curvilinear symmetry coordinates as follows:

$$\phi_{1ss} = \frac{1}{hc} \left(\frac{h}{4\pi^2 c} \right)^{3/2} (\omega_1 \omega_s^2)^{-1/2} \sum_r \sum_{r'} \tilde{f}_{1rr} L_{11} L_{rs} L_{r's} + \tilde{f}_{rr'} (2L_r^{1s} L_{r's} + L_r^{ss} L_{r'1}) + \dots \quad (8)$$

L_r^{ss} and L_r^{1s} can be written explicitly in terms of L_{11} and L_{rs} . In both methods [Eqs. (4) and (6)] we calculate $\langle Q_s^2 \rangle$ as $(h/8\pi^2 c \omega_s) \coth(hc\omega_s^{\text{obs}}/2kT)$.

We have also estimated the mean bond displacements by using Bartell's simple method for AX_n-type molecules.¹³ In this method the contributions to $\langle \Delta r \rangle$ are a sum of Morse, nonbonded, bending, and minor shrinkage and correction terms. For AX₆ they are

$$\begin{aligned} \langle \Delta r \rangle_{\text{Morse}} &= (3a/2)(K/f_{11})\langle (\Delta r)^2 \rangle, \\ \langle \Delta r \rangle_{\text{nonbonded}} &= -(F_3/f_{11} r_e)\langle (\Delta q)^2 \rangle, \\ \langle \Delta r \rangle_{\text{bend}} &= (2f_\alpha/f_{11} r_e)\langle (r\Delta\alpha)^2 \rangle, \\ \langle \Delta r \rangle_x &= (4\sqrt{2}/f_{11})(F'K_{xx} + F\delta_{xx}) \\ &\quad - (1/f_{11} r_e)(F' + F)\langle (r\Delta\alpha) \rangle^2, \\ \langle \Delta r \rangle_{\text{rot}} &= 2E_{\text{rot}}/6f_{11} r_e = kT/2f_{11} r_e. \end{aligned} \quad (9)$$

This is an approximate version of the full calculation by the Bartell method in Eqs. (2) and (3).

The results are shown in Tables III–VI. For SF₆ there are several anharmonic force fields available. We provide the comparison in Table VI as an indication of the sensitivity of the empirical $(\partial\sigma^F/\partial\Delta r)_e$ values obtained to the force field used. We calculated these using all three methods. The use of Bartell's coupled equations as expressed by Eqs. (2) and (3) and the L tensor method as expressed by Eqs. (5)–(7) give identical results. The curvilinear correction to $\langle \Delta r \rangle$, that part which is due to the nonlinear transformation between internal and normal coordinates, arises from the quadratic part of the force field and is independent of the anharmonic

TABLE III. Contributions to the mean bond displacement and its temperature dependence, all in 10⁻³ Å.

	³² SF ₆	⁸⁰ SeF ₆ ^b	¹³⁰ TeF ₆ ^c	¹⁸⁴ WF ₆ ^d	Pt ³⁵ Cl ₆ ⁼	Pt ⁷⁹ Br ₆ ⁼
$\langle \Delta r \rangle^{300}$	7.506	6.479	6.618	4.725	7.890	10.173
Vib.	7.314	6.259	6.410	4.556	7.531	9.756
Quad. ^a	0.859	0.824	0.716	0.565	1.129	1.269
Rot.	0.192	0.220	0.208	0.170	0.359	0.417
a_1^e	7.41E-3	8.60E-3	9.19E-3	8.99E-3	2.08E-2	3.06E-2
a_2^f	1.16E-5	1.18E-5	1.13E-5	6.33E-6	8.37E-6	5.45E-6
$\langle (\Delta r)^2 \rangle^{300}$	1.7318	1.5940	1.5123	1.4777	2.8231	2.7431
b_1^f	9.21E-4	1.11E-3	1.10E-3	1.11E-3	6.53E-3	7.55E-3
b_2^f	2.59E-6	3.14E-6	3.04E-6	3.00E-6	4.26E-6	2.61E-6
$\Delta_T = \langle \Delta r \rangle^{400} - \langle \Delta r \rangle^{200}$	1.490	1.709	1.829	1.792	4.139	6.113
Rot.	0.128	0.147	0.139	0.113	0.240	0.278

^a The quadratic contributions to $\langle \Delta r \rangle_{\text{vib}}$ are due to the nonlinear transformation between Δr and the normal coordinates, which gives a nonzero $\langle \Delta r \rangle$ even when the cubic force constants in curvilinear internal coordinates are zero. $\langle \Delta r \rangle = \langle \Delta r \rangle_{\text{vib}} + \langle \Delta r \rangle_{\text{rot}}$; $\langle \Delta r \rangle_{\text{vib}} = \langle \Delta r \rangle_{\text{cub}} + \langle \Delta r \rangle_{\text{quad}}$.

^b For ⁷⁷SeF₆ the values are $\langle \Delta r \rangle^{300} = 6.489 \times 10^{-3}$ Å, $\Delta_T = 1.706 \times 10^{-3}$ Å.

^c For ¹²⁵TeF₆ the values are $\langle \Delta r \rangle^{300} = 6.626 \times 10^{-3}$ Å, $\Delta_T = 1.826 \times 10^{-3}$ Å.

^d For ¹⁸³WF₆ the values are nearly the same, $\langle \Delta r \rangle^{300} = 4.726 \times 10^{-3}$ Å, and $\Delta_T = 1.792 \times 10^{-3}$ Å.

^e $\langle \Delta r \rangle^T = \langle \Delta r \rangle^{300} + a_1(T - 300) + a_2(T - 300)^2$.

^f $\langle (\Delta r)^2 \rangle^T = \langle (\Delta r)^2 \rangle^{300} + b_1(T - 300) + b_2(T - 300)^2$.

TABLE IV. Mass dependence of the mean bond displacements in octahedral molecules at 300 K.^a

m_{MF_6}	m' (amu)	$\Delta_M = \langle \Delta r \rangle_{m_{\text{MF}_6}} - \langle \Delta r \rangle_{m_{\text{MF}_6}}$ (10^{-5} Å)
⁷⁴ SeF ₆ $\langle \Delta r \rangle = 6.501 \times 10^{-3}$ Å	82	2.883
	80	2.211
	78	1.509
	77	1.146
	76	0.773
¹²² TeF ₆ $\langle \Delta r \rangle = 6.632 \times 10^{-3}$ Å	130	1.371
	128	1.044
	126	0.706
	125	0.534
	124	0.359
	123	0.181
¹⁸² WF ₆ $\langle \Delta r \rangle = 4.727 \times 10^{-3}$ Å	186	0.304
	184	0.154
	183	0.077

$$^a \langle \Delta r \rangle_{\text{Pt}^{13}\text{Cl}_6^-} - \langle \Delta r \rangle_{\text{Pt}^{11}\text{Cl}_6^-} = 3.891 \times 10^{-5} \text{ Å}; \quad \langle \Delta r \rangle_{\text{Pt}^{18}\text{Br}_6^-} - \langle \Delta r \rangle_{\text{Pt}^{17}\text{Br}_6^-} = 0.900 \times 10^{-5} \text{ Å}.$$

model used. For SF₆ this is 8.6×10^{-4} Å at 300 K, to be compared with the total $\langle \Delta r \rangle$ which is 7.506×10^{-3} Å, that is, approximately 10%. The curvilinear correction to the isotope effect on $\langle \Delta r \rangle$ at 300 K is approximately 10% in these molecules. Using the L tensor method we find that $\langle \Delta \alpha \rangle = 0$. We had made this assumption in the implementation of Bartell's method in Eq. (3) in order to solve 6 coupled equations with no redundancies rather than 18 with redundancies.

Bartell's simple method [Eq. (9)] provides $\langle \Delta r \rangle$ values that are within 96% of the full calculations, as can be seen in comparing Tables III–IV with Table V. Here the nonlinear transformation contribution to $\langle \Delta r \rangle$ is largely in the bend contributions and in the small shrinkage and correction terms. The latter and the rotational contribution to $\langle \Delta r \rangle$ are small in all cases. For all the molecules studied here the values obtained by this approximation for $\langle \Delta r \rangle$ and its changes with mass and temperature are 93%–105% of those obtained by the full calculation. Considering the simplicity of making these estimates, the results are surprisingly good compared to the full calculations.

In Fig. 1 we compare our calculations for SF₆ with the electron diffraction data of Kelley and Fink.¹⁴ The agreement with experiment is reasonably good for the Krohn–Overend (KO) and the Stanton–Bartell (SB) potential. The force field by Hodgkinson *et al.* includes only cubic force constants f_{rrr} , f_{rrr}^{cis} , f_{rrr}^{trans} . The mean bond displacements obtained with this are smaller, indicating that interactions described by $f_{rr\alpha}$, $f_{r\alpha\alpha}$, etc., give nonnegligible contributions to $\langle \Delta r \rangle$. Indeed the Hodgkinson force field gives a temperature dependence of $\langle \Delta r \rangle$ that is substantially smaller than that obtained in the electron diffraction experiments.¹⁴ The KO and SB force fields give satisfactory descriptions of the latter experiment.

APPLICATIONS TO NMR PARAMETERS

The isotope shifts and temperature coefficients of ¹⁹F shielding can be interpreted with the use of the mean bond displacements from these tables. For symmetry-conserving isotopic substitution in these octahedral molecules, $\langle \Delta r \rangle_{\text{rot}}$ is independent of mass. The M-induced ¹⁹F isotope shift at 300 K is given by

$$^1\Delta^{19}\text{F}(m'/m) \equiv \sigma(m_{\text{MF}_6}) - \sigma(m_{\text{MF}_6}). \quad (10)$$

This can be written in terms of the derivatives of the shielding and the mass dependence of the mean M–F bond displacement:

$$^1\Delta^{19}\text{F}(m'/m) \approx \left(\frac{\partial \sigma^{\text{F}}}{\partial \Delta r} \right)_e [\langle \Delta r \rangle_{\text{vib}} - \langle \Delta r \rangle'_{\text{vib}}] + \frac{1}{2} \left(\frac{\partial^2 \sigma^{\text{F}}}{\partial \Delta r^2} \right)_e [\langle (\Delta r)^2 \rangle - \langle (\Delta r)^2 \rangle'] + \dots \quad (11)$$

The temperature dependence of the chemical shift is given by

$$\sigma_0^{\text{F}}(T) - \sigma_0^{\text{F}}(300 \text{ K}) \approx (\partial \sigma^{\text{F}} / \partial \Delta r)_e \{ \langle \Delta r \rangle^T - \langle \Delta r \rangle^{300} \} + \frac{1}{2} (\partial^2 \sigma^{\text{F}} / \partial \Delta r^2)_e \{ \langle (\Delta r)^2 \rangle^T - \langle (\Delta r)^2 \rangle^{300} \} + \dots \quad (12)$$

Similarly, for the shielding of the central atom in MX₆,

$$^1\Delta^{\text{M}}(m'/m) \approx \left(\frac{\partial \sigma^{\text{M}}}{\partial \Delta r} \right)_e \cdot 6 [\langle \Delta r \rangle - \langle \Delta r \rangle'] + \frac{1}{2} \times (\partial^2 \sigma^{\text{M}} / \partial \Delta r^2)_e \cdot 6 [\langle (\Delta r)^2 \rangle - \langle (\Delta r)^2 \rangle'] + \dots \quad (13)$$

TABLE V. Mean bond displacements (Å) calculated with Bartell's approximate method.

	³² SF ₆	⁸⁰ SeF ₆	¹³⁰ TeF ₆	Pt ³⁵ Cl ₆ [−]
$\langle \Delta r \rangle^{300}$	5.812×10^{-3}	6.256×10^{-3}	6.450×10^{-3}	7.890×10^{-3}
% ^a	(42,50,5,3)	(51,40,5,4)	(62,30,5,3)	(50,38,7,5)
$\langle \Delta r \rangle^{400} - \langle \Delta r \rangle^{200}$	1.182×10^{-3}	1.609×10^{-3}	1.743×10^{-3}	4.183×10^{-3}
%	(22,63,4,11)	(28,56,8,9)	(33,49,9,8)	(44,42,8,6)
$\langle \Delta r \rangle - \langle \Delta r \rangle'$	2.46×10^{-5}	2.75×10^{-5}	1.32×10^{-5}	3.99×10^{-5}
	(³² S – ³⁴ S)	(⁷⁴ Se – ⁸² Se)	(¹²² Te – ¹³⁰ Te)	(³⁵ Cl – ³⁷ Cl)
%	(81,0,19,0)	(91,0,9,0)	(96,0,4,0)	(71,26,3,0)

^a Percent contributions from Morse, nonbonded, quadratic, and rotation, respectively, as given by Eq. (9).

TABLE VI. Comparison of different force fields for SF_6 .

	Krohn and Overend ^a	Stanton and Bartell ^b	Hodgkinson ^c
$\langle \Delta r \rangle^{300}, 10^{-3} \text{ \AA}$	7.506	6.057	5.359
$\Delta_T = \langle \Delta r \rangle^{400} - \langle \Delta r \rangle^{200}, 10^{-3} \text{ \AA}$	1.490	1.272	0.878
$\Delta_M = \langle \Delta r \rangle^{74\text{SF}_6} - \langle \Delta r \rangle^{74\text{SeF}_6}, 10^{-5} \text{ \AA}$	3.40	2.60	0.90

^a Reference 1.^b Reference 2.^c Reference 3.

and

$$\begin{aligned} \sigma_0^M(T) - \sigma_0^M(300 \text{ K}) \\ \approx \left(\frac{\partial \sigma^M}{\partial \Delta r} \right)_e \cdot 6[\langle \Delta r \rangle^T - \langle \Delta r \rangle^{300}] \\ + \frac{1}{2} \left(\frac{\partial^2 \sigma^M}{\partial \Delta r^2} \right)_e \left\{ 6[\langle (\Delta r)^2 \rangle^T - \langle (\Delta r)^2 \rangle^{300}] + \dots \right. \end{aligned} \quad (14)$$

One interesting result is shown in Fig. 2. In the preceding paper we observed that the isotope shift ${}^1\Delta^{19}\text{F}(m'/m\text{Se})$ is directly proportional to $(m' - m)/m'$, a mass factor which arose empirically from a vibrational analysis of CH_4 , CD_4 , and CT_4 isotopomers.¹⁵ We find here that this empirical relationship is well expressed by the result of the calculations which verify the proportionality of $[\langle \Delta r \rangle^{74\text{SeF}} - \langle \Delta r \rangle^{m'\text{SeF}}]$ and $[\langle (\Delta r)^2 \rangle^{74\text{SeF}} - \langle (\Delta r)^2 \rangle^{m'\text{SeF}}]$ to the factor $(m' - 74)/$

m' , as shown in Fig. 2. That the direct proportionality to $(m' - m)/m'$ is obtained exactly for the calculated $\langle \Delta r \rangle$ and $\langle (\Delta r)^2 \rangle$ and also for the observed chemical shift is an indication that bond angle deformations play no important role in isotope shifts in this type of molecule. A similar result is observed in Fig. 2 for the Te-F bond in TeF_6 , which explains the observed mass dependence of ${}^1\Delta^{19}\text{F}(m'/{}^{122}\text{Te})$. Although the isotope shift is too small to observe in WF_6 [we predict ${}^1\Delta^{19}\text{F}({}^{186}/{}^{182}\text{W})$ to be ≤ 0.005 ppm], it can be assumed that a similar behavior to Fig. 2 of the preceding paper will be observed at much higher magnetic fields.

If the terms in the second derivatives of shielding in Eqs. (11)–(14) are neglected, the ratio of $\sigma_0(T_2) - \sigma_0(T_1)$ to the isotope shift can be related to the calculated rovibrational averages. For example,

$$\left[\frac{{}^1\Delta^{19}\text{F}(m'/m\text{M})}{\sigma_0^F(T_2) - \sigma_0^F(T_1)} \right]_{\text{obs}} \approx \left[\frac{\langle \Delta r \rangle - \langle \Delta r \rangle'}{\langle \Delta r \rangle^{T_2} - \langle \Delta r \rangle^{T_1}} \right]_{\text{calc}} \quad (15)$$

A similar equation can be written for the shielding of the central atom in MF_6 . In general, for MX_n molecules, the

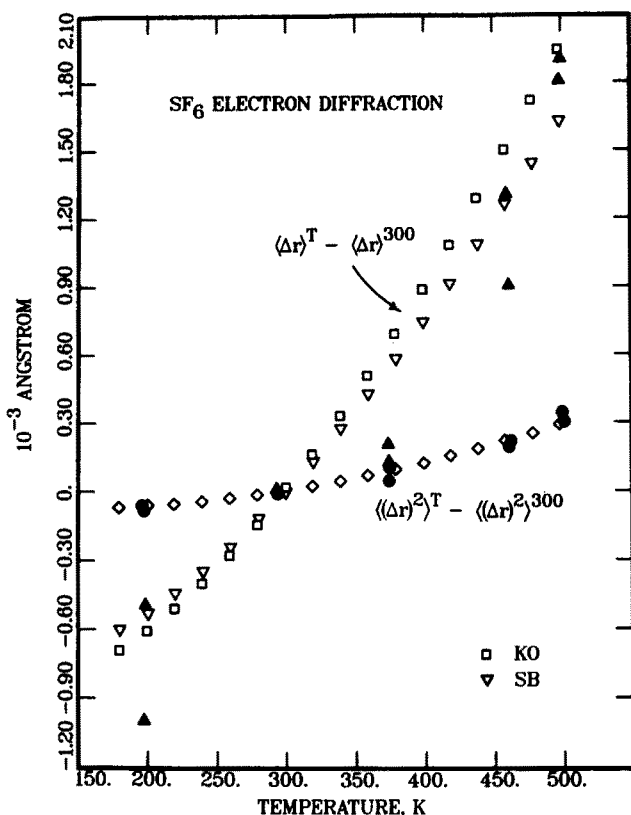


FIG. 1. Comparison of calculated mean bond displacements and mean square amplitudes of the S-F bond in SF_6 with the experimental results of Kelley and Fink (Ref. 14).

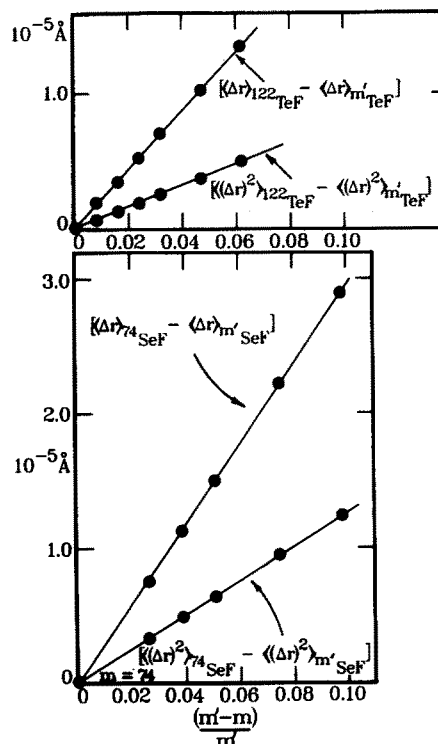


FIG. 2. Calculated mass dependence of the mean bond displacements and mean square amplitudes (at 300 K) of the Se-F and Te-F bonds in SeF_6 and TeF_6 . The mass factor $(m' - m)/m'$ is discussed in the text.

dynamic calculations on isotopomers $^{p'/p}M^{q'/q}X_n$ are approximately related to the NMR observables as follows:

$$\frac{\langle \Delta r \rangle_p - \langle \Delta r \rangle_{p'}}{\langle \Delta r \rangle_{T_2} - \langle \Delta r \rangle_{T_1}} \approx \frac{{}^1\Delta X({}^{p'/p}M)}{\sigma_0^X(T_2) - \sigma_0^X(T_1)}, \quad (16)$$

$$\frac{\langle \Delta r \rangle_q - \langle \Delta r \rangle_{q'}}{\langle \Delta r \rangle_{T_2} - \langle \Delta r \rangle_{T_1}} \approx \frac{{}^1\Delta M({}^{q'/q}X)}{\sigma_0^M(T_2) - \sigma_0^M(T_1)}. \quad (17)$$

In Eq. (17) both the experiment and the calculations pertain to the M^qX_n molecule and the *fully substituted* $M^{q'}X_n$.

In principle, given both the observed isotope shift and the temperature dependence of the shielding in the isolated molecule, the two parameters $(\partial\sigma/\partial\Delta r)_e$ and $(\partial^2\sigma/\partial\Delta r^2)_e$ can be determined from a fitting of the experimental NMR results to the calculated $\langle \Delta r \rangle^T$ and $\langle (\Delta r)^2 \rangle^T$ functions. In practice this is possible only if the anharmonic force field gives sufficiently accurate mass and temperature dependence of $\langle \Delta r \rangle^T$ and $\langle (\Delta r)^2 \rangle^T$, and negligible contributions from $\langle (\Delta\alpha)^2 \rangle^T$ and other terms. Although both $\langle \Delta r \rangle_{\text{vib}}$ and $\langle (\Delta r)^2 \rangle$ depend on the same set of $\coth(hc\omega_{\text{obs}}/2kT)$ functions, $\langle \Delta r \rangle_{\text{rot}}$ is proportional to temperature in the classical limit. Thus, $\langle \Delta r \rangle^T$ has less curvature than $\langle (\Delta r)^2 \rangle^T$. Comparison of the experimental temperature dependence of shielding in the isolated molecules with the temperature dependence of $\langle \Delta r \rangle^T$ and $\langle (\Delta r)^2 \rangle^T$ shows that $(\partial\sigma/\partial\Delta r)_e < 0$ and $(\partial^2\sigma/\partial\Delta r^2)_e < 0$. To obtain physically reasonable first and second derivatives we can examine the family of curves with *relative* contributions from the $\langle \Delta r \rangle$ and $\langle (\Delta r)^2 \rangle$ terms. For a given choice of

$$n \equiv \frac{(\partial^2\sigma/\partial\Delta r^2)_e}{(\partial\sigma/\partial\Delta r)_e}$$

it is possible to find the best one-parameter fit of the experimental temperature dependence of the chemical shift to $A_n\{\langle \Delta r \rangle^T + (n/2)\langle (\Delta r)^2 \rangle^T\}$. The best fit value of A_n is an empirical estimate of $(\partial\sigma/\partial\Delta r)_e$. In Fig. 3 we show the fits to experiment^{4,16} for $n = 0$. When $n \neq 0$, the $(\partial^2\sigma/\partial\Delta r^2)_e \langle (\Delta r)^2 \rangle^T$ term tends to bring the more nearly linear $(\partial\sigma/\partial\Delta r)\langle \Delta r \rangle^T$ function to closer agreement with the apparent curvature of the experimental data. However, the differences between the calculated curves for $n = 0$ to 4 \AA^{-1} are not visible in this scale. The curvature of the calculated $n = 10 \text{ \AA}^{-1}$ curve is only very slightly in the direction of better agreement with the experimental curvature. The best fit parameters obtained for $n = 0$ are summarized in Table VII. Shielding derivatives can also be calculated from the observed isotope shifts.^{4,17} The results are shown in Table VII. These shielding derivatives are comparable to the values obtained for C–F bonds in various fluoromethanes.¹⁸ An earlier estimate of $(\partial\sigma/\partial\Delta r)_e$ in SF_6 was $-2200 \text{ ppm \AA}^{-1}$.¹⁹ This was based on the simple Bartell model, Eq. (9), with slightly different force field anharmonicity. Improved models for anharmonic force fields tend to give larger values of $\langle \Delta r \rangle$. We expect the values in Table VII to be modified as more complete information about anharmonicities in these molecules become available.

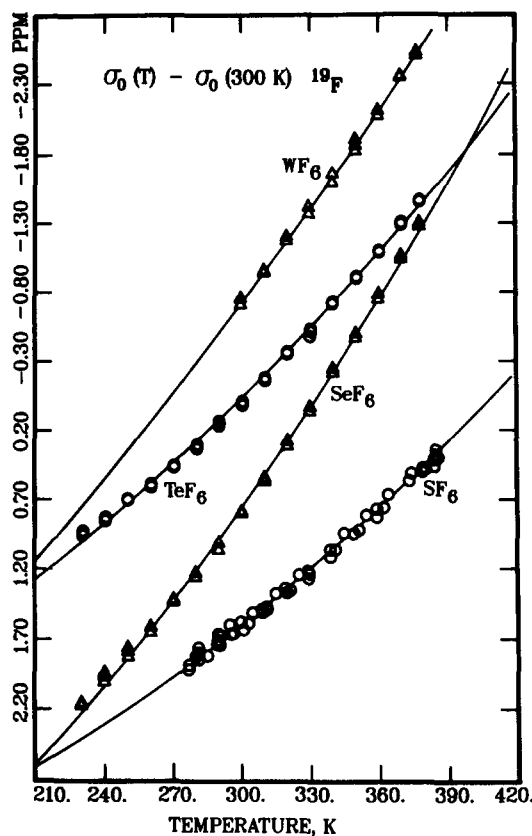


FIG. 3. Comparison of the observed temperature dependence [$\sigma_0(T) - \sigma_0(300 \text{ K})$] of ^{19}F in octahedral fluorides with the calculated curves $(\partial\sigma/\partial\Delta r)_e [\langle \Delta r \rangle^T - \langle \Delta r \rangle^{300}]$, using $(\partial\sigma/\partial\Delta r)_e \approx -1930, -2690, -1770$, and -2500 ppm/\AA for $\text{SF}_6(\text{SB})$, SeF_6 , TeF_6 , and WF_6 , respectively. (Except for TeF_6 , the individual plots are arbitrarily offset for display.)

NMR PARAMETERS OF THE CENTRAL ATOM

The temperature dependence of the ^{77}Se and ^{125}Te chemical shifts in SeF_6 and TeF_6 can be interpreted with the same $\langle \Delta r \rangle^T$ as the ^{19}F data, using Eq. (14). The one-parameter fit to the data for these nuclei is shown in Fig. 4; these yield the shielding derivatives shown in Table VII and estimates of the rovibrational corrections [$\sigma_0(300) - \sigma_e$] for ^{77}Se and ^{125}Te shielding.

In PtCl_6^- and PtBr_6^- ions for isotope shifts ${}^1\Delta^{195}\text{Pt}(^{37/35}\text{Cl}) = -0.167 \text{ ppm per } ^{37}\text{Cl}$ and ${}^1\Delta^{195}\text{Pt}(^{81/79}\text{Br}) = -0.028 \text{ ppm per } ^{81}\text{Br}$ have been reported.²⁰ From the present calculations of the mass dependence and temperature dependence of $\langle \Delta r \rangle$ we can estimate with Eq. (14) a temperature coefficient for the ^{195}Pt chemical shift in PtCl_6^- : $-0.53 \text{ ppm deg}^{-1}$. Although this quantity has not been measured for PtCl_6^- , the temperature coefficient of the ^{195}Pt chemical shift in $\text{Pt}(\text{R}_3\text{P})_2\text{Cl}_4$ has been reported as $-0.6 \text{ ppm deg}^{-1}$ (*cis*) and $-0.85 \text{ ppm deg}^{-1}$ (*trans*).²¹ PtCl_6^- is more shielded than these other complexes.²² On the basis of our previous work on temperature coefficients of ^{19}F shielding in fluoromethanes²³ and binary fluorides⁴ which show a correlation between ^{19}F shielding and their temperature coefficients, the more shielded ^{195}Pt in PtCl_6^- is expected to have a somewhat smaller temperature

TABLE VII. Shielding derivatives and rovibrational corrections to shielding in MX₆-type molecules.

	Mass range	From isotope shift		T range	From T dependence	
		$(\partial\sigma/\partial\Delta r)_e^c$ ppm Å ⁻¹	$\sigma_0(300) - \sigma_e$ ppm		$(\partial\sigma/\partial\Delta r)_e^c$ ppm Å ⁻¹	$\sigma_0(300 \text{ K}) - \sigma_e$ ppm
¹⁹ F in SF ₆ ^a	32–34	– 1560	– 12	280–380	– 1640	– 12
¹⁹ F in SF ₆ ^b	32–34	– 2040	– 12	280–380	– 1930	– 12
¹⁹ F in SeF ₆	74–82	– 2000	– 13	230–380	– 2690	– 17
¹⁹ F in TeF ₆	122–130	– 1080	– 7	230–380	– 1770	– 12
¹⁹ F in WF ₆				300–380	– 2500	– 12
⁷⁷ Se in SeF ₆				300–380	– 1500	– 8
¹²⁵ Te in TeF ₆				310–380	– 1050	– 7
¹⁹⁵ Pt in PtCl ₆ [–]	35–37	– 4300	– 340			
¹⁹⁵ Pt in PtBr ₆ [–]	79–81	– 3100	– 320			

^a Using anharmonic force field from Krohn and Overend (Ref. 1). The best fit to *both* is obtained with $(\partial\sigma/\partial\Delta r)_e \approx -1600 \text{ ppm } \text{\AA}^{-1}$ and $(\partial^2\sigma/\partial\Delta r^2)_e \approx 0$.

^b Using anharmonic force field from Stanton and Bartell (Ref. 2). The best fit to *both* is obtained with $(\partial\sigma/\partial\Delta r)_e \approx -1890 \text{ ppm } \text{\AA}^{-1}$ and $(\partial^2\sigma/\partial\Delta r^2)_e \approx -560 \text{ ppm } \text{\AA}^{-2}$.

^c See the Appendix.

coefficient than $-0.6 \text{ ppm deg}^{-1}$. For PtBr₆[–] we can make a similar estimate $d\sigma^{\text{Pt}}/dT \approx -0.57 \text{ ppm deg}^{-1}$. The ¹⁹⁵Pt shielding derivatives and rovibrational corrections to shielding estimated from the isotope shifts are shown in Table VII.

DISCUSSION

The empirical estimates of shielding derivatives from isotope shifts and the temperature shifts differ. The difference is a measure of the limitations of the anharmonic model as well as the approximations inherent in the calculation (neglect of other second derivatives and use of harmonic

oscillator partition functions) and experimental errors. Except for the SB field for SF₆, the values of the isotope shifts calculated from the best-fit parameters obtained from the temperature dependence are all too large for any *n* (0 to 10.0). The observed isotope shifts are 61%, 74%, and 95% of the calculated values of ¹Δ for TeF₆, SeF₆, and SF₆ (KO) for *n* = 0 and the discrepancy worsens with higher *n*.

We find that the ratio of the mass-dependent and temperature-dependent chemical shifts ¹Δ/[σ₀(T₂) – σ₀(T₁)] is a sensitive test of the anharmonic force field, given the precision with which these quantities can be measured. The anharmonic force fields used here for SeF₆ and TeF₆ give too small values of [$\langle\Delta r\rangle^{T_2} - \langle\Delta r\rangle^{T_1}$] or too large values of [$\langle\Delta r\rangle - \langle\Delta r\rangle'$] or both. The result is that a fit to the temperature dependence gives too large an isotope shift and a fit to the isotope shift gives a temperature coefficient that is too small. The calculated ratio in Eq. (15) is outside the combined experimental errors in the observed ¹Δ/[σ₀(T₂) – σ₀(T₁)] for ¹⁹F in SeF₆ and TeF₆. For SF₆ both the SB and KO force fields can account for the shape of the temperature dependent chemical shift function fairly well with only the term in the first derivative, and the curvature is quite well reproduced. A good fit to *both* the isotope shift and the temperature dependence is obtained with the SB force field equally well with $(\partial\sigma/\partial\Delta r)_e \approx -2000 \text{ ppm } \text{\AA}^{-1}$ and $(\partial^2\sigma/\partial\Delta r^2)_e \approx 0$ as with $(\partial\sigma/\partial\Delta r)_e \approx -1890 \text{ ppm } \text{\AA}^{-1}$ and $(\partial^2\sigma/\partial\Delta r^2)_e \approx -560 \text{ ppm } \text{\AA}^{-2}$ (see the Appendix). The best fit for the KO force field is obtained with only the first derivative term with an average value of $(\partial\sigma/\partial\Delta r)_e \approx -1600 \text{ ppm } \text{\AA}^{-1}$. The derivatives for WF₆, PtCl₆[–], and PtBr₆[–] have unknown errors because we only have one type of NMR measurement, the quadratic force fields for these Pt complexes, and the Morse and other parameters are not as well established as for the other molecules. Measurements of the temperature shifts of the ¹⁹⁵Pt shielding in these complexes would help to put bounds on the shielding derivatives, but only if additional vibrational spectroscopic data becomes available to better define the anharmonic force fields for these ions.

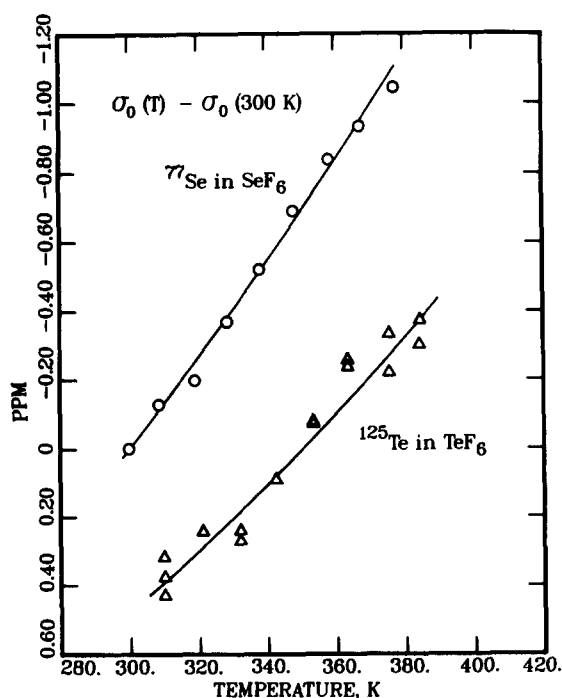


FIG. 4. Comparison of the observed temperature dependence of ⁷⁷Se and ¹²⁵Te shielding in SeF₆ and TeF₆ with the same [$\langle\Delta r\rangle^{T_2} - \langle\Delta r\rangle^{300}$] as used in Fig. 3, with $(\partial\sigma/\partial\Delta r)_e \approx -1500$ and $-1300 \text{ ppm}/\text{\AA}$, respectively, for ⁷⁷Se and ¹²⁵Te. The TeF₆ curve is displaced by 0.5 ppm.

It is interesting that in the related series of molecules, SF₆, SeF₆, TeF₆, the largest derivative is for ¹⁹F in SeF₆. We have previously noted that the paramagnetic term in the perpendicular component of ¹⁹F shielding provides the greatest contribution to $(\partial\sigma^F/\partial\Delta r)_e$ in HF molecule.²⁴ The diamagnetic term in shielding is known to change less drastically with bond extension, not just in HF but in other molecules as well.²⁵ The paramagnetic contributions to the parallel and perpendicular components of ¹⁹F shielding have been measured in SF₆, SeF₆, and TeF₆. They are: $\sigma_{\parallel}^F = -770$, -924 , and -857 ppm, $\sigma_{\perp}^F = -256$, -204 , -191 ppm, respectively.²⁶ We have found here that the shielding derivative is largest for the environment with the largest σ_{\parallel}^F , SeF₆ [although the ordering of $(\partial\sigma/\partial\Delta r)$ for SF₆ and TeF₆ is not strictly in agreement with the ordering of σ_{\parallel}^F].

CONCLUSIONS

Although the mean bond displacements calculated here have been applied specifically to the interpretation of the temperature and mass dependence of NMR parameters, the same treatment can be used for other molecular electronic properties such as electric dipole polarizability, magnetic susceptibility, electric multipole moments, etc. The high resolution, reproducibility, and availability of multiple probe nuclei which the NMR method provides make the chemical shift a good test of anharmonic force fields.

In this paper we have verified the equivalence of the Bartell and the *L* tensor methods for calculating mean bond displacements. We have shown that for SF₆ the SB and KO force fields are in agreement with the electron diffraction data on hot SF₆ molecules. The explanation of the observed strict proportionality of the isotope shifts $^1\Delta X^{(m'/m)M}$ to the mass factor $(m' - m)/m'$ in MF₆ molecules has been found in the proportionality of both $[\langle\Delta r\rangle - \langle\Delta r\rangle']$ and $[\langle(\Delta r)^2\rangle - \langle(\Delta r)^2\rangle']$ to the same mass factor. We find that a combination of NMR observables, the isotope shifts, and temperature shift of the shielding, provides a severe test of anharmonic fields. In a single parameter fitting, the obtained parameter can be interpreted as a combination of first and second derivatives. Unfortunately, the force fields for the molecules studied here are do not allow the individual determinations to be made. Nevertheless, the signs of the shielding derivatives have been established and the $\langle\Delta r\rangle$ term by itself gives calculated ratios of NMR observables which are of the correct order of magnitude: 61%, 74%, 95%, and 105% of the observed ratios for TeF₆, SeF₆, SF₆, (KO), and SF₆ (SB).

ACKNOWLEDGMENT

This research was supported in part by the National Science Foundation (Grant No. CHE85-05725).

APPENDIX

Since $\langle\Delta r\rangle$ and $\langle(\Delta r)^2\rangle$ change with temperature (and mass) in the same direction, the single parameter obtained from fitting either the temperature dependence or the mass dependence of chemical shifts using only $A_0\langle\Delta r\rangle$ can be interpreted as

$$A_0 = \left(\frac{\partial\sigma}{\partial\Delta r} \right)_e \left(1 + \frac{1}{2} nx_T \right), \quad (18)$$

$$A'_0 = \left(\frac{\partial\sigma}{\partial\Delta r} \right)_e \left(1 + \frac{1}{2} nx_m \right), \quad (19)$$

where

$$n \equiv \frac{(\partial^2\sigma/\partial\Delta r^2)_e}{(\partial\sigma/\partial\Delta r)_e}$$

and

$$x_T = \frac{\langle(\Delta r)^2\rangle^{T_2} - \langle(\Delta r)^2\rangle^{T_1}}{\langle\Delta r\rangle^{T_2} - \langle\Delta r\rangle^{T_1}},$$

$$x_m = \frac{\langle(\Delta r)^2\rangle - \langle(\Delta r)^2\rangle'}{\langle\Delta r\rangle - \langle\Delta r\rangle'}.$$

For the empirical shielding derivatives given in Table VII the values of x_m calculated from the force fields used are 0.416, 0.543, 0.427, 0.353, 0.490, 0.501, and 0.452 Å for SF₆ (KO), SF₆ (SB), SeF₆, TeF₆, WF₆, PtCl₆[−], and PtBr₆[−], respectively. It is seen in Table V that the M mass dependence of $\langle\Delta r\rangle$ in MF₆ molecules (but not the X mass dependence of $\langle\Delta r\rangle$ in MX₆) is largely due to the Morse stretching anharmonicity, so that $x_m \approx 2f_{11}/3aK$. The calculated values of x_m are 75%, 86%, and 93% of $2f_{11}/3aK$ for SF₆, SeF₆ and TeF₆, respectively. The calculated values of x_T for the temperature ranges in Table VII are 0.132, 0.156, 0.128, 0.119, and 0.142 Å for ³²SF₆ (KO), ³²SF₆ (SB), ⁸⁰SeF₆, ¹³⁰TeF₆, and ¹⁸⁴WF₆, respectively. In the favorable situation where the anharmonic force field is sufficiently well defined to give good values of x_T and x_m , then the two parameters obtained by separately fitting the temperature dependence of the chemical shift in the isolated molecule and the isotope shifts could be interpreted as in Eqs. (18) and (19) to provide a unique value of *n*, thereby providing an empirical determination of both $(\partial\sigma/\partial\Delta r)_e$ and $(\partial^2\sigma/\partial\Delta r^2)_e$. For example, the SB field for SF₆ gives $A'_0 = -2040$ ppm Å^{−1}, $A_0 = -1930$ ppm Å^{−1}, which lead to $n = 0.30$ and $(\partial\sigma/\partial\Delta r)_e \approx -1890$ ppm Å^{−1}, $(\partial^2\sigma/\partial\Delta r^2)_e \approx -560$ ppm Å^{−2}.

¹B. J. Krohn and J. Overend, *J. Phys. Chem.* **88**, 564 (1984).

²J. F. Stanton and L. S. Bartell, *J. Phys. Chem.* **89**, 2544 (1985).

³D. P. Hodgkinson, J. C. Barrett, and A. G. Robiette, *Mol. Phys.* **54**, 927 (1985).

⁴C. J. Jameson, A. K. Jameson, and D. Oppusungu, *J. Chem. Phys.* **85**, 5480 (1986).

⁵L. S. Bartell, *J. Mol. Struct.* **63**, 259 (1981).

⁶J. Kestin, S. T. Ro, and W. A. Wakeham, *Physica* **58**, 165 (1972).

⁷J. Hiraishi, I. Nakagawa, and T. Shimanouchi, *Spectrochim. Acta* **20**, 819 (1964).

⁸P. LaBonville, J. R. Ferraro, M. C. Wall, and L. J. Basile, *Coord. Chem. Rev.* **7**, 257 (1972).

⁹D. R. Herschbach and V. W. Laurie, *J. Chem. Phys.* **35**, 458 (1961).

¹⁰L. S. Bartell, *J. Chem. Phys.* **38**, 1827 (1963); **70**, 4581 (1979).

¹¹C. J. Jameson and H. J. Osten, *J. Chem. Phys.* **81**, 4915, 4288 (1984).

¹²A. R. Hoy, I. M. Mills, and G. Strey, *Mol. Phys.* **24**, 1265 (1972).

¹³L. S. Bartell, *J. Chem. Phys.* **70**, 4581 (1979); L. S. Bartell, S. K. Doun, and S. R. Goates, *ibid.* **70**, 4585 (1979).

¹⁴M. H. Kelley and M. Fink, *J. Chem. Phys.* **27**, 1813 (1982).

¹⁵C. J. Jameson and H. J. Osten, *J. Chem. Phys.* **81**, 4293 (1984).

¹⁶C. J. Jameson, A. K. Jameson, and S. M. Cohen, *J. Chem. Phys.* **67**, 2771 (1977).

¹⁷R. J. Gillespie and J. W. Quail, *J. Chem. Phys.* **39**, 2555 (1963).

- ¹⁸C. J. Jameson and H. J. Osten, *Mol. Phys.* **55**, 383 (1985).
¹⁹C. J. Jameson, *Mol. Phys.* **40**, 999 (1980).
²⁰I. M. Ismail, S. J. J. Kerrison, and P. J. Sadler, *J. Chem. Soc. Chem. Commun.* **1980**, 1175.
²¹T. H. Brown and S. M. Cohen, *J. Chem. Phys.* **58**, 395 (1973).
²²R. J. Goodfellow, in *Multinuclear NMR*, edited by J. Mason (Plenum, New York, 1986).
²³C. J. Jameson, *Mol. Phys.* **54**, 73 (1985).
²⁴C. J. Jameson and H. J. Osten, *Ann. Rep. NMR Spectrosc.* **17**, 1 (1986).
²⁵R. D. Amos, *Mol. Phys.* **39**, 1 (1980); *Chem. Phys. Lett.* **68**, 536 (1979).
²⁶S. K. Garg, J. A. Ripmeester, and D. W. Davidson, *J. Magn. Reson.* **39**, 317 (1980).
²⁷Y. M. Bosworth, R. J. H. Clark, and D. M. Rippon, *J. Mol. Spectrosc.* **46**, 240 (1973).
²⁸R. S. McDowell and L. B. Asprey, *J. Mol. Spectrosc.* **48**, 254 (1973).
²⁹Y. M. Bosworth and R. J. H. Clark, *J. Chem. Soc. Dalton Trans.* **1974**, 1749.
³⁰F. Königer, A. Müller, and H. Selig, *Mol. Phys.* **34**, 1629 (1977).
³¹S. Abramovitz and I. W. Levin, *J. Chem. Phys.* **44**, 3353 (1966).
³²H. M. Seip and R. Seip, *Acta Chem. Scand.* **20**, 2698 (1966).
³³G. Engel, *Z. Kryst.* **90**, 343 (1935).
³⁴D. L. Hildenbrand, *J. Chem. Phys.* **62**, 3074 (1975).